DOLOČITEV DINAMIČNIH ZEMELJSKIH TLAKOV DELUJOČIH NA TOGE PREPUSTE: PREIZKUSI NA POTRESNIH MIZAH

Deniz Ulgen *(vodilni avtor)*
Mugla Sitki Koçman University,
Faculty of Engineering, Department of Civil Engineering
48100 Mugla, Turčija
E-pošta: denizulgen@mu.edu.tr

Mehmet Yener Ozkan
Middle East Technical University,
Faculty of Engineering, Department of Civil Engineering
06800 Ankara, Turčija
E-pošta: myozkan@metu.edu.tr

Ključne besede

škatlasti prepust, dinamični zemeljski pritisk, potresna miza, dinamična interakcija tla-konstrukcija, laminarna škatla, dinamični bočni koeficient

Izvleček

Potresna varnost podzemnih objektov (prepusti, podzemne železnice, sistemi za oskrbo z zemeljskim plinom in vodo), igra pomembno vlogo v trajnostni javni varnosti in urbanem razvoju. Ne poznamo splošno sprejetega postopka za oceno dinamičnih pritiskov, ki delujejo na podzemne objekte. Prav tako je na voljo zelo malo eksperimentalnih podatkov za oceno dinamičnih pritiskov. S študijo želimo izboljšati razumevanje dinamičnega obnašanja škatlastih prepustov in pritiskov, ki delujejo pri dinamičnih vzbujanjih s pomočjo eksperimentalnih analiz. V ta namen smo izvedli niz preizkusov na potresni-mizi na škatlastih prepustih zakopanih v suhem pesku. Za simulacijo robnih pogojev prostega polja, smo za uporabo v 1 g potresni mizi zasnovali in izdelali laminarno škatlo. Na dveh modelih prepustov, ki imata različne togosti smo v raznih harmoničnih gibanjih preučili vpliv razmerja prožnosti na vrednosti dinamičnih bočnih pritiskov tal. Na podlagi rezultatov preskusov predlagamo poenostavljeno porazdelitev dinamični pritiskov, ki delujejo na stranske stene modela prepusta. Za predlagano vrhnjo vrednost tlaka v porazdelitvi tlakov smo definirali dinamični bočni koeficient. Vrednosti tega koeficienta so funkcija strižnih specifičnih deformacij z upoštevanjem relativne togosti med tlemi in podzemno konstrukcijo.

EVALUATION OF DYNAMIC SOIL PRESSURES ACTING ON RIGID CULVERTS: SHAKING-TABLE TESTS

Deniz Ulgen *(corresponding author)*
Mugla Sitki Koçman University,
Faculty of Engineering, Department of Civil Engineering
48100 Mugla, Turkey
E-mail: denizulgen@mu.edu.tr

Mehmet Yener Ozkan
Middle East Technical University,
Faculty of Engineering, Department of Civil Engineering
06800 Ankara, Turkey
E-mail: myozkan@metu.edu.tr

Abstract

The seismic safety of underground structures (culvert, subway, natural-gas and water-sewage systems) plays a major role in sustainable public safety and urban development. Very few experimental data are currently available and there is no generally accepted procedure to estimate the dynamic pressures acting on these underground structures. This study aims to enhance the state of the prevalent information necessary to understand the dynamic behaviour of box culverts and the stresses acting under dynamic excitations through experimental analyses. For this purpose, a series of shaking-table tests were conducted on box-type culverts buried in dry sand. To simulate the free-field boundary conditions, a laminar box was designed and manufactured for use with a 1-g shake table. Two culvert models having different rigidities were tested under various harmonic motions in order to examine the effect of the flexibility ratio on dynamic lateral soil pressures. Based on the test results, a simplified dynamic pressure distribution acting on the sidewalls of the culvert model was suggested. Then, a dynamic lateral coefficient was defined for the proposed peak pressure value in the distribution. The values of this coefficient were obtained as a function of the shear strain by considering the relative stiffness between the soil and the underground structure.

1 INTRODUCTION

The seismic design and safety of buried structures including pipelines, culverts, subways and tunnels are crucial requirements for economic and infrastructure development. The seismic assessment of underground structures gained more importance after the heavy damage from large earthquakes such as 1995 Kobe, Japan; 1999 Kocaeli, Turkey; and 1999 Chi Chi, Taiwan. The 1995 Hyogo-ken Nanbu (Kobe) Earthquake of magnitude M_w=6.9 occurred in the northern part of Awaji island near Kobe, Japan. It was one of the most destructive earthquakes and caused significant damage to Kobe's underground rapid transit system [1]. The extensive damage occurred in the Daikai Subway station built using the cut-and-cover technique. It was mentioned that the collapse of the subway and the intense damage were caused by the earthquake forces. Iida et al. [2] presented their observations from Daikai Station after the Kobe earthquake and explained the damage and failure mechanism in the subway tunnel. It was observed that shear cracks occurred on the walls of the station during the earthquake. The authors pointed out that the relative movement between the station and the overburden soil could be the main reason for the collapse. Parra-Montesinos et al. [3] evaluated the

collapse of the Daikai Subway Station and focused on the soil–structure interactions. It was emphasized that the friction between the structure and soil, the soil degradation and the relative movement between the soil and the structure should be taken into account in the design of underground structures against earthquakes. Wang et al. [4], Shimizu et al. [5], Wang and Zhang [6] and Shen et al. [7] assessed the damage mechanism of mountain tunnels under earthquake loading. It was observed that tunnels buried at shallow depths or near the surface experienced significant damage as compared to the deeply embedded tunnels. Furthermore, it was concluded that the tunnels should be constructed far away from the surface slopes and active faults. Hashash et al. [8] reviewed the several reported case histories of underground structures prepared by Duke and Leeds [9], Stevens [10], Dowding and Rozen [11], Owen and Scholl [12], Sharma and Judd [13], Power et al. [14], Kaneshiro et al. [15], In these case histories, the San Francisco Bay area rapid transit system, the Alameda tubes in California, the Los Angeles metro, the underground structures in Kobe, Japan, the underground structures in Taiwan, and the Bolu tunnel were investigated.

Ground shaking is produced by seismic waves including body waves and surface waves. Body waves are categorized as compressional and shear waves. Shear waves are the most destructive form of body waves that cause ovaling or racking deformation of underground structures [16, 8]. Within the scope of this study, the dynamic response of the underground structures was examined by producing vertically propagating shear waves.

Seismic deformations may be underestimated or overestimated depending on the relative stiffness between the buried structure and the surrounding ground [16]. In order to take into account the soil–structure interaction effect, simplified frame analysis (SFA) methods are proposed by Wang [16], Penzien [17], Huo et al. [18] and Bobet et al. [19]. Another approach to evaluating the seismic design of underground structures is the force-based method. In this method, equivalent seismic forces caused by the inertial force of the soil under earthquake loading are estimated. There is no generally accepted approach to predicting the dynamic soil pressures exerted on a culvert. One widely preferred approach to predicting the dynamic earth pressures acting on the embedded structures is the Mononobe-Okabe method [20,21]. It is not reasonable to use the Mononobe-Okabe method for rectangular buried structures since a yielding active wedge does not usually occur in the surrounding soil during an earthquake. Wang [16] stated that the Mononobe Okabe approach can be applied to structures having a U-section or buried near the soil surface. He emphasized that as the structure's embedment depth increased the theory tended

to overestimate the racking deformations. Moreover, Luu [22] employed shaking-table tests and reported that the Mononobe Okabe approach gave inconsistent values for the soil's dynamic pressures.

Nishiyama et al. [23] performed shaking-table tests in order to investigate the friction between the soil and the underground structure. In the study it was pointed out that shear stresses at the ceiling and normal pressures acting on the sidewalls decrease with the decreasing friction between the ground and the embedded structure. Che and Iwatate [24] conducted shaking-table tests and numerical analyses to evaluate the dynamic lateral earth pressures and bending strains exerted on the underground structure. The authors concluded that the lateral earth pressures due to vertical motions could be ignored and rocking motions were observed during the horizontal motion. Matsui et al. [25] investigated the seismic performance of two span rectangular underground reinforced-concrete structures by employing large shaking-table experiments. The results of the study showed that the centre of the wall tended to deform inward owing to dynamic soil pressures. Bending cracks occurred at the top and bottom of the outer surface and uniform horizontal cracks were observed on the inner surface of the sidewall due to inward deformations. In later research, Che et al. [26] carried out shaking-table tests and observed that the absolute dynamic earth-pressure values were nearly identical to the values obtained from static analyses. Moreover, it was mentioned that the normal strain of the culvert could be ignored. Moss and Crosariol [27] studied the dynamic response of rigid underground structures buried in soft clay using shaking-table tests. The authors stated that the racking deformations were highly dependent on the input accelerations and that the racking deformations increased linearly with an increase of the accelerations. Chen et al. [28] performed shaking-table tests on a subway structure in soft soil and reported that the underground structures and soil were more sensitive to the low-frequency components of strong ground motions.

The ovaling deformation mode of underground structures was evaluated by Cilingir & Madabushi [29], Cilingir & Madabushi [30] and Lanzano et al. [31]. These studies mainly concentrated on the embedment depth, the dynamic soil pressures and the acceleration response of the soil. There are only a few researches [32-34] assessing the racking deformation and dynamic response of buried rectangular underground structures. Pitilakis et al. [33] performed centrifuge tests to examine the dynamic response of rectangular tunnels buried in soft soils. Results showed that the dynamic pressures acting at the centre of the sidewall were smaller than the pressures acting near the corners of the flexible tunnel.

There is a lack of experimental data for evaluating the dynamic response of rectangular underground structures. Thus, more research is required in order to clarify the seismic effects on a buried structure. In this study, 1-g shaking-table tests were performed to investigate the dynamic earth pressures acting on the box-type underground culvert. The effect of the relative stiffness between the buried culvert and the surrounding ground was evaluated under harmonic motions. Moreover, the influence of acceleration on the dynamic behaviour of the underground box-type culvert was examined. The tests provided a better understanding of the qualitative behaviour of box-type embedded structures subjected to dynamic loading. As a consequence, the main objective of this study is to make a reasonable contribution, to help to understand the dynamic load-transfer mechanism between the soil and the box-type underground culverts.

2 SHAKING-TABLE TEST SYSTEM

Shaking-table tests were carried out in the dynamic laboratory of the Civil Engineering Department of Middle East Technical University. The shaking-table system was mounted on the main steel frame having plan dimensions of 3.5 m × 1 m. The main frame was connected to a reinforced concrete foundation by welding the anchor plates. The whole system was designed and constructed by Calisan [35]. There were three main parts of the shaking-table system, i.e., the motion-generating system (actuators), the model container and the data-acquisition system. In the present study, the system was modified by using a motor driver and a laminar box. A motor driver was added to the motion-generating system to adjust the frequencies and to obtain a soft start during the shaking. Furthermore, a laminar box was designed and fabricated in the Ostim Organized Industry. The maximum displacement limit of the motion-generating system is 6 mm and the frequency range is 0.5–10 Hz. The peak accelerations used in the tests vary from 0 to 0.5 g.

2.1 Design of the Soil container

A rigid container does not conform to the soil deformation pattern and generate P-waves during shaking. Therefore, the available rigid system was renovated by using a laminar box instead of a rigid box so as to eliminate the boundary effects (Prasad et al. [36], Turan et al. [37], Hokmabadi [38]) in the current study. A rectangular laminar container was preferred rather than a ring-type container considering the plain-strain conditions for a box-type underground structure. A

typical laminar box is constructed of several horizontal rectangular metal frames stacked together. The frames are free to move on linear roller bearings in the direction of motion. Thus, the box is able to conform to the soil-deformation pattern during shaking. The stiffness resisting the movement of the soil is the friction between the layers and the linear roller bearings. For this reason, the main purpose in the design of the laminar box is to minimize the friction as much as possible. Within the scope of this study, a laminar box (Fig. 1a) was designed and manufactured in the Ostim Organized Industry. It is rectangular in cross-section with dimensions of 1 m (width) × 1.5 m (length) × 1 m (height). The box is composed of nine rectangular steel frames. Each frame is 10-cm deep and the spacing between the frames is 1 cm. There are linear bearings connected to the outside rigid supporting frame on the long side (Fig. 1b). The linear bearings are fixed in a transverse direction, while they are free to move in the longitudinal direction. The short sides of the laminar frames (Fig. 1c) are connected to the long sides by means of hinge joints allowing rotation in
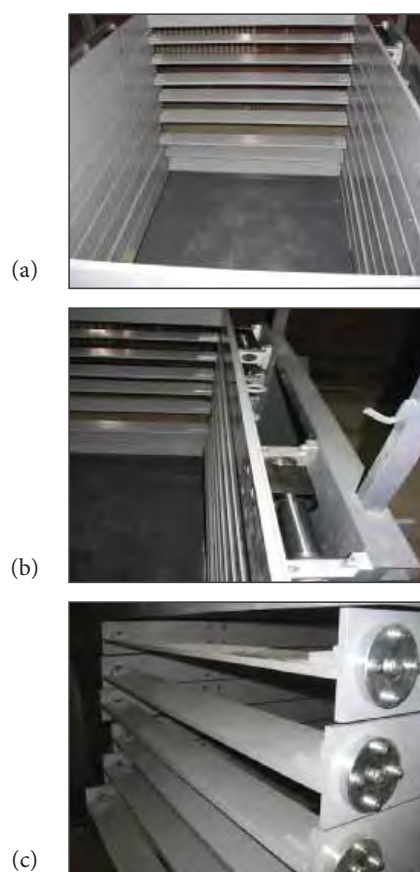

(a)

(b)

(c)

Figure 1. General view of the laminar box (b) Linear bearing connected to outside rigid supporting frame (c) Short side of the laminar box.

a transverse direction. Hence, the sidewalls of the box conform to soil-deformation and the boundary effects are minimized. The shaking table carries the ground model that was covered with a membrane to prevent soil leakage from the spacings between the laminar layers. There is no contact between the shaking table and the soil container. The shaking table vibrates the ground model and the laminar box conforms to the deformation scheme of the ground model.

2.2 Soil properties

Air dried Çine sand was used to construct the model ground in the shaking-table tests. Based on the Unified Soil Classification System (USCS), the soil can be identified as SP: poorly graded, slightly silty, medium sand. The grain size distribution curve of the sand was determined through a dry-sieve analysis. The parameters derived from distribution curve are as follows: Table 1 shows the physical properties of Çine sand.

Table 1. Physical properties of Çine sand used in shaking table tests.

Specific gravity	2.66	Coefficient of uniformity (C_u)	3.53
Minimum void ratio	0.44	Coefficient of curvature (C_c)	0.92
Maximum void ratio	0.80	Mean diameter (D_{50}) (mm)	0.45
Minimum unit weight (kN/m^3)	14.50	Fines content (%)	1.15
Maximum unit weight (kN/m^3)	18.10	Poisson's Ratio	0.3

Direct shear and triaxial tests were conducted to find the shear-strength parameters of the soil. The normal stress range in the direct shear and triaxial tests changes between 14 kPa and 50 kPa. A disturbed test sample was taken from the dry Çine sand and placed into triaxial test apparatus at a relative density of 60%. Çine sand has a friction angle of 42° at that relative density.

Initially, the maximum shear modulus was estimated as 20000 kPa using Eq.1, proposed by Hardin and Drnevich [39]. Next, the model ground was modelled in the one-dimensional ground-response analyses program SHAKE91 and the results were calibrated with the obtained free-field shear strains at the mid-depth of the culvert in shaking-table tests. Fig. 2 shows the shear modulus reduction (G/G_{max}) obtained from back-analyses of the free-field shaking-table results

using SHAKE91. The shear-modulus degradation curve proposed by Darendeli [40] is given in the same figure for reference. The curve was plotted for a mean effective stress (3.6 kPa) representing the stress levels of the culvert depths in the shaking-table tests. G_{max} is the initial (low-strain) shear modulus and G is the shear modulus at any strain level. After the calibration, for a relative density of 60%, the maximum shear modulus of the ground surrounding the culvert was predicted to be 13,000 kPa.

$$G_{max} = 3230 \cdot \frac{(2.973 - e)^2}{(1 + e)} \cdot OCR^k \cdot (\sigma'_m)^{1/2} \qquad (1)$$
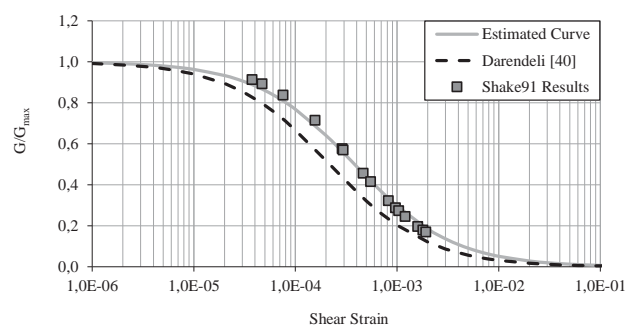

Figure 2. Variation of normalized shear modulus with respect to shear strain.

2.3 Preparation of model ground

The raining method [41] was used to prepare the model ground throughout the shaking-table tests. In order to obtain a homogeneous model ground and a uniform density throughout the laminar box, sand was pluviated into the laminar box from a height of 60cm using a sieve. The sieve is rectangular in cross-section with dimensions of 0.98 m (width) × 1.48 m (length) and a mesh size of 2.36 mm. When constructing the model ground, first, a sand bed with a thickness of 20 cm was placed into the box in two layers and compacted with a vibration tamper in order to represent a bearing stratum. Later, the remaining part of the sand was placed into the laminar box in layers of 10-cm thickness by pluviation to simulate a cut-and-cover tunnel model. During the sand raining, five small boxes were buried in the soil at different locations to determine the relative density of the sand. Measurements with small boxes showed that a uniform density and homogeneous ground model can be obtained by sand pluviation. The relative densities of the sand bed and the overlying sand changed by 80–85% and 60–65%, respectively.

2.4 Box-type culvert models

Two different types of box culvert models were used in the shaking-table tests. The box models were made of steel, which was selected as a suitable material for the culvert model among multiple alternatives such as aluminium, wood and concrete. Thus, the culvert model can be easily processed and thinner rigid walls can be obtained. Each model is 20 cm × 20 cm in cross-section and the side walls of the box structure models have two kinds of thickness, i.e., 5 mm and 10 mm. The culvert was placed into the laminar box in the transverse direction. The length of the culvert model is 80 cm. Hence, there is a friction between the culvert and the soil particles. The extremities of the culvert were lubricated

to decrease the friction. The culverts were labelled as *C1* and *C2*, respectively. The upper and lower slabs of the culvert models were relatively thick and rigid, compared to sidewalls. Thus, dynamic lateral earth pressures can be monitored by eliminating the structural effects due to the bending of the slabs. Cross-sections of the box models are illustrated in Fig. 3.

The box models were manufactured by considering the flexibility ratio, which represents the relative stiffness between the soil and the structure. The flexibility ratio of a single barrel box can be directly calculated by using the equation proposed by Wang [16]. The equation (Eq. 2) is given by:

$$F = \frac{G_s}{24}\left(\frac{H^2 W}{EI_W} + \frac{HW^2}{EI_R} \right) \qquad (2)$$

where G_s is the shear modulus of the soil, H is the height and W is the width of the box structure, I_W is the moment of inertia of the walls, and I_R is the moment of inertia of the slabs. The physical meaning of the F (flexibility ratio) values can be described as follows: for $F>1$, the structure is more flexible than the soil and for $F<1$ the structure is more rigid than the soil.

The configuration of the structure model and the layout of the transducers are depicted in Fig. 4. The box culvert model was buried in sand at a depth of 40 cm. In order to minimize the boundary effects caused by the laminar
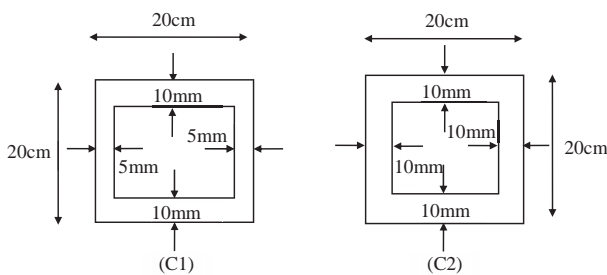

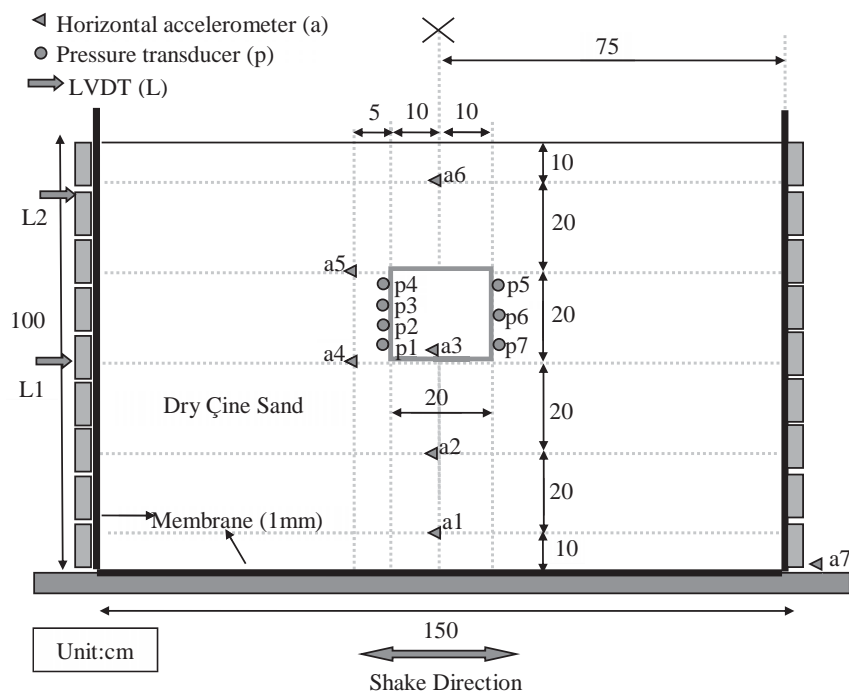**Figure 3**. Cross-sections of the steel culvert models used in the shaking-table tests.

Figure 4. Layout of the culvert model and the numbering of the transducers.

box, the model and transducers were placed in the middle of the container. Seven pressure transducers were mounted on the box model to measure the dynamic soil pressures. Five accelerometers were buried in the ground model to determine the soil accelerations and deformations, and one accelerometer was placed on the shaking table to measure the input motion. Two displacement transducers (LVDT) were connected to a rigid, stable, outside frame at heights of 50 cm and 90 cm. The technical parameters of the transducers are given Table 2.

Table 2. Main technical parameters of the transducers.

Transducer	Acceleration	Pressure	Pressure	Displacement
Type	ARF-10A	KDF-200KPA	Honeywell AB/HP	SDP-100C
Capacity	$10m/s^2$	200kPa	42kPa	100mm
Rated output	0.5mv/v	0.3mv/v	1mv/v	2.5mV/V
Nonlinearity	1%	1%	0.5%	0.2%
Operating temperature	-10° C to 50° C	-20° C to 60° C	-54° C to 93° C	0° C to 60° C
Allowable excitation voltage	5V	10V	5V	5V
Weight	13g	160g	57g	350g

3 TESTING PROGRAM AND PROCEDURE FOR SHAKING-TABLE TESTS

There were a total of 33 shaking-table tests performed under different harmonic motions having various acceleration amplitudes and frequencies. The model ground was constructed for each test, hence, the input motions were applied separately for each test. Thus, the initial physical state is almost the same for each test. The testing program included different cases given as follows:

- Free-field response tests
- Model tests for two different culvert models (*C1*, *C2*), when the model was buried at a depth of 40 cm.

The testing program applied for all the culvert models can be tabulated as shown in Table 3.

4. RESULTS AND DISCUSSION

4.1 Boundary effect of laminar box

The boundary effect of the laminar container on the ground motion was investigated by using accelerometers. One accelerometer (a6) was placed near the sidewall at a distance of 5 cm from the membrane and the other accelerometer (a3) was placed in the middle of the laminar container. Both accelerometers were at the same level, at the mid-height of the laminar box. The acceleration time histories at those locations were recorded during the shaking-table tests. The results indicate that the acceleration record near the sidewall is very similar to the acceleration record in the middle of the container. There was almost no phase difference between the acceleration time histories; only the amplitudes changed. The ratio of the acceleration amplitude near the sidewall to the acceleration amplitude at the centre, ar, was plotted against the input acceleration in Fig. 5. As seen in Fig. 5,

Table 3. Testing program applied in shaking table experiments.

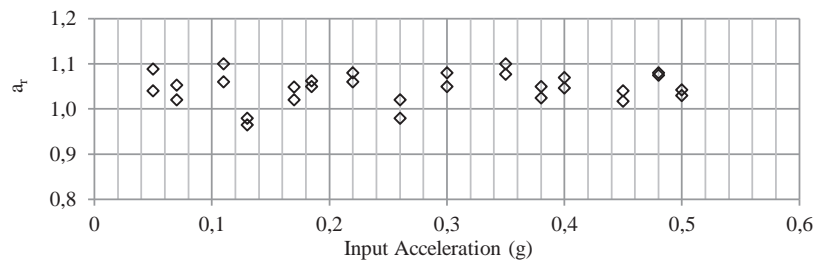|	Free Field			Culvert Model 1 (*C1*)			Culvert Model 2 (*C2*)	
Test No	Acceleration (g)	Frequency (Hz)	Test No	Acceleration (g)	Frequency (Hz)	Test No	Acceleration (g)	Frequency (Hz)
1	0.05	2.0	12	0.05	2.0	23	0.05	2.0
2	0.07	2.0	13	0.07	2.0	24	0.07	2.0
3	0.11	3.1	14	0.11	3.1	25	0.11	3.1
4	0.17	3.1	15	0.17	3.1	26	0.17	3.1
5	0.22	3.1	16	0.22	3.1	27	0.22	3.1
6	0.26	4.2	17	0.26	4.2	28	0.26	4.2
7	0.30	4.2	18	0.30	4.2	29	0.30	4.2
8	0.35	5.3	19	0.35	5.3	30	0.35	5.3
9	0.40	5.3	20	0.40	5.3	31	0.40	5.3
10	0.45	6.4	21	0.45	6.4	32	0.45	6.4
11	0.50	6.4	22	0.50	6.4	33	0.50	6.4

Figure 5. Variation of acceleration amplitude ratio (wall to centre), a_r, with respect to the input acceleration.

there is a minor variation of about 5% and 10% between the wall and the centre accelerations. Hence, it can be said that the walls of the laminar container do not have a significant boundary effect on the ground motion. In this study, the model was placed at the centre of the container to minimize the boundary effects.

4.2 Comparison of measured static lateral coefficients with Jaky's formula

Fig. 6 shows the variation of the lateral earth-pressure coefficients (K) with respect to the depth ratio. The depth ratio is represented by d/H, where d is the distance from the pressure transducer to the upper corner of the culvert and H is the culvert height. For comparison, two lines indicating the at-rest and the active earth-pressure coefficients, K_o and K_a, were drawn in the same plot. K_o was calculated from the following empirical relationship (Eq. 3) proposed by Jaky [42]:

$$K_o = 1 - \sin\phi' \qquad (3)$$

where ϕ' is the drained friction angle. K_a was determined using Eq. 4, suggested by Rankine [43]. For an internal friction angle of 42°, K_o and K_a were calculated as 0.33 and 0.2, respectively.

$$K_a = \frac{1 - \sin\phi'}{1 + \sin\phi'} \qquad (4)$$

As seen from Fig. 6, all the measured earth-pressure coefficient values are above the K_a line. The K values obtained for the culvert models *C1* and *C2* are in close agreement with the K_o line. The results showed that the lateral earth-pressure coefficient decreased with an increasing flexibility ratio, as expected. The sidewall of the flexible culverts deforms more than that of the rigid culverts and accordingly the walls are subjected to a low soil pressure.

4.3 Maximum acceleration along the depth of the ground model

In order to investigate the variation of the maximum acceleration along the depth of the soil model, the accelerometers were placed at 5 different depths in the soil, as shown in Fig. 7. The recorded maximum accelerations at those depths normalized with the maximum shaking acceleration and plotted versus the soil depth as given in Fig. 8a and Fig. 8b. As seen in Fig. 8a, the normalized acceleration (amplification ratio) is very low and changes around 1 for the maximum input accelerations 0.05 g, 0.07 g, and 0.11 g. This means that the soil behaves as a
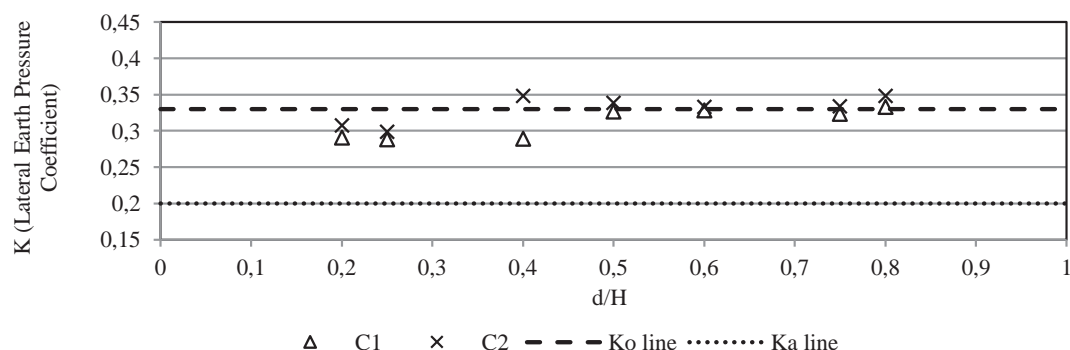

Figure 6. Variation of the earth-pressure coefficient (K) with respect to the depth ratio (d/H).
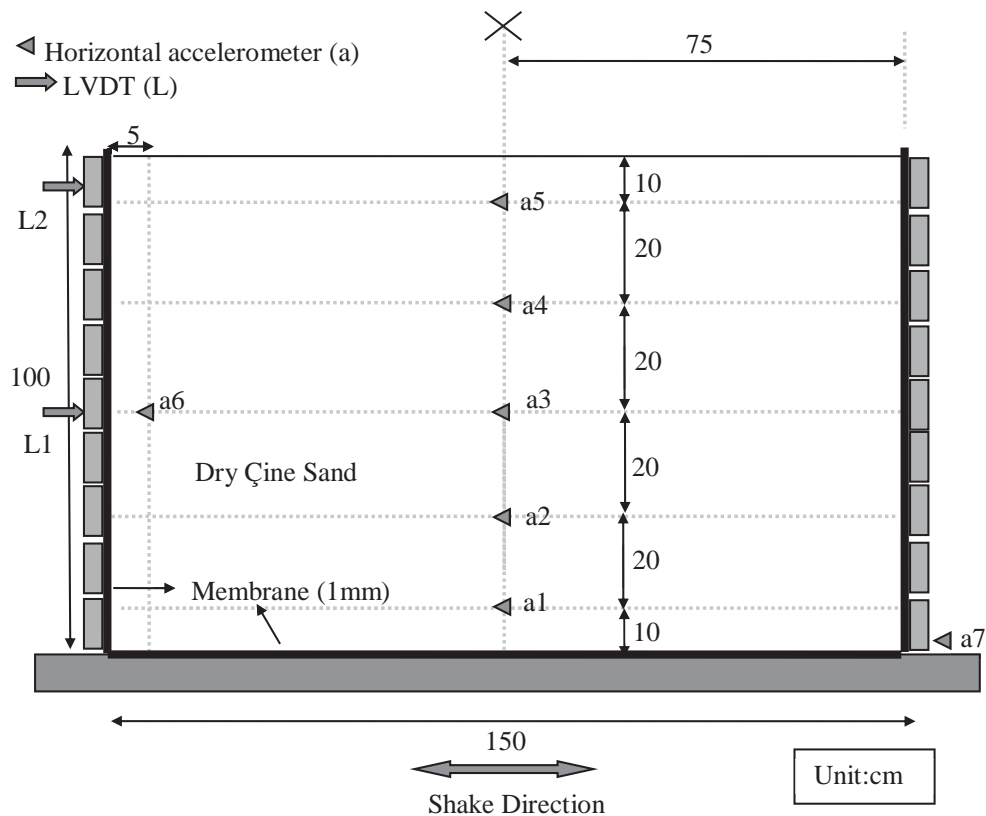
Figure 7. Layout of the transducers in free-field shaking-table tests.

rigid mass at low strain levels. The amplification ratio starts to increase at 0.17 g and at the top layer of the soil it becomes approximately 1.1 g. Fig. 8b shows the variation of the normalized acceleration along the depth of the soil model for the maximum input accelerations of 0.22 g, 0.26 g, 0.30 g, 0.34 g, 0.4 g, 0.45 g and 0.50 g. In the figure, it is observed that the amplification ratio near the surface changes between 1.2 and 1.4. Higher accelerations in the upper region of the model ground may occur due to reflection and refraction of the seismic waves from the surface.

4.4 Evaluation of displacements and shear strains

The displacement of the laminar box and the soil were measured by using linear variable transducers and accelerometers, respectively. The LVDT measures the displacements directly. In contrast to the LVDT, the accelerometer can provide an indirect measure of the displacement by integrating the acceleration time history twice. Before the integration process the data must be filtered to prevent any unwanted errors or misleading results. For this reason, the recorded acceleration time histories were filtered by a bandpass filter between 1Hz and 20Hz (high

pass at 1 Hz and low pass at 20Hz). Thus, high-frequency noise and drift due to spurious low-frequency components were eliminated to enhance the data quality.

The accelerometers were placed at different heights in the soil model. As explained above, the displacements were computed by a double integration of the acceleration records. Assuming that the displacement is varying linearly between the two accelerometers located at points 1 and 2, the shear strain can be calculated using Eq. 5:

$$\gamma = \frac{d_2 - d_1}{z_2 - z_1} \qquad (5)$$

where γ is the shear strain, d_1, d_2 are the displacements at points 1, 2 and z_1, z_2 are the heights at points 1, 2, respectively. Based on this approach, the soil's shear strain around the culvert model was obtained for the input motions having different acceleration amplitudes. Two displacement transducers, $L1$ and $L2$, were placed at mid height (50 cm elevation) and near the top (90 cm elevation) of the laminar box. The displacement time histories were analysed at different acceleration levels, i.e., 0.11 g and 0.4 g. It was observed that the
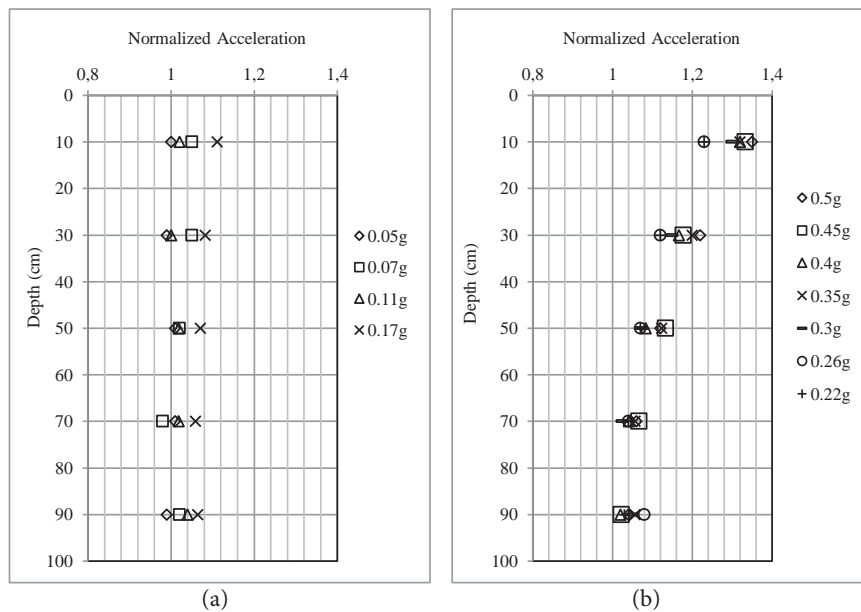
Figure 8. Variation of the maximum acceleration along the soil profile for maximum input accelerations (a) For 0.05 g, 0.07 g, 0.11 g, 0.17 g (b) For 0.22 g, 0.26 g, 0.3 g, 0.35 g, 0.4 g, 0.45 g, 0.5 g.

relative displacement between $L1$ and $L2$ increases with an increase in the acceleration, as expected. Moreover, there is a small phase shift at higher accelerations. The following figures (Fig. 9, Fig. 10) provide a comparison between the displacement time histories recorded by $L1$ and $L2$ for different accelerations.
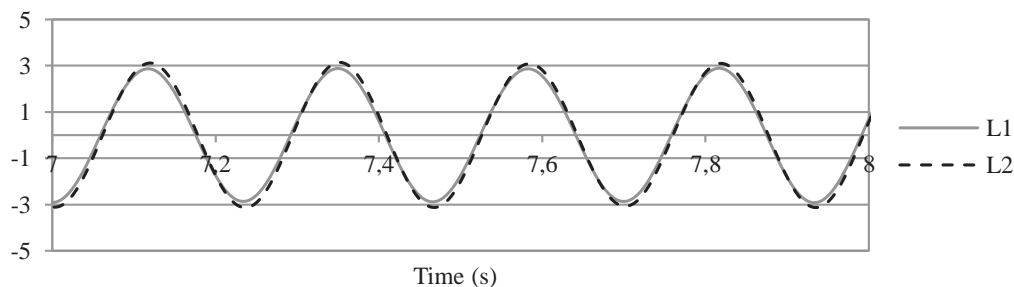

Figure 9. Displacement time histories recorded by $L1$ and $L2$ at 0.11 g maximum input acceleration.
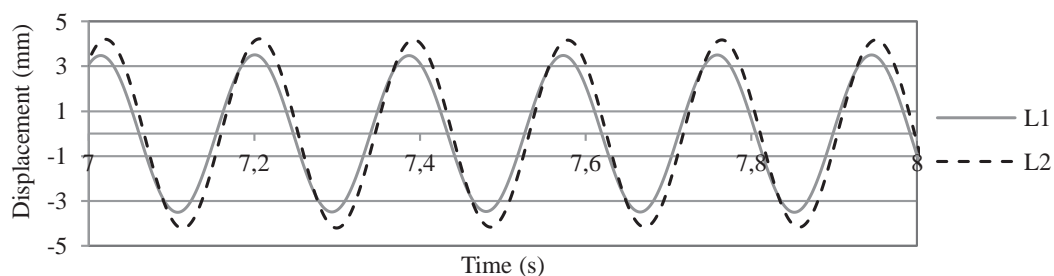

Figure 10. Displacement time histories recorded by $L1$ and $L2$ at 0.4 g maximum input acceleration.

4.5 Determination of the flexibility ratio for the culvert models

The flexibility ratio (relative stiffness) is defined as the ratio of the soil stiffness to the structural stiffness. It has a significant role on the dynamic response of the under-ground culverts; hence special attention should be given to the determination of the flexibility ratio. In dynamic soil culvert interaction analyses the relative stiffness is represented by the ratio of the shear modulus of the surrounding ground to the structural racking (flexural) stiffness. The main difficulty in determining the flex-ibility ratio is the assessment of shear modulus, which is strongly dependent on the intensity of the dynamic motion. It decreases with the increasing shear strain of the soil. Therefore, different flexibility ratios can be obtained under different dynamic motions for the same culvert. Based on this conclusion, the flexibility ratios of the two culvert models were determined at different strain levels. The three-step procedure for calculating the flexibility ratios is as follows:

1) The shear strain at the mid-depth of the culvert model was computed from the accelerometer records of a4 and a5 using Eq. 5.
2) The degraded shear modulus at the calculated shear strain in step 1 was obtained using Fig. 2.
3) The calculated shear modulus in step 2 was substitu-ted into Eq. 2 to obtain the flexibility ratio.

Table 4 presents the flexibility ratio values for both of the culvert models at different input accelerations.

4.6 Dynamic soil pressures acting on the sidewalls of the culverts

In the shaking-table tests the lateral soil pressures were measured at each sidewall of the culvert models. During the tests the static and dynamic pressures were measured separately. For this purpose, first, the static pressure was recorded, then the dynamic pressures were measured by taking the initial values as static pressures. There are four pressure transducers on the left-hand side and three pressure transducers on the right-hand side of the culvert model. Fig. 11 and Fig. 12 show the variation of the recorded maximum dynamic pressures at those sensors with respect to the free field shear strain (at the mid-depth of the culvert) for the two culvert models used in the shaking-table tests.

The maximum pressures at each cell were measured at different times during the excitation. In other words, they do not act on the sidewalls of the culvert, simultaneously. As seen from the figures the maximum dynamic pressure increases with an increase of the shear strain and the rigidity of the structure, as expected. Moreover, it was observed that the maximum dynamic pressures occur near the corners of the culvert model. Dynamic lateral soil pressures acting on the sidewalls of

Table 4. Flexibility ratio values for the culvert models at different input accelerations.

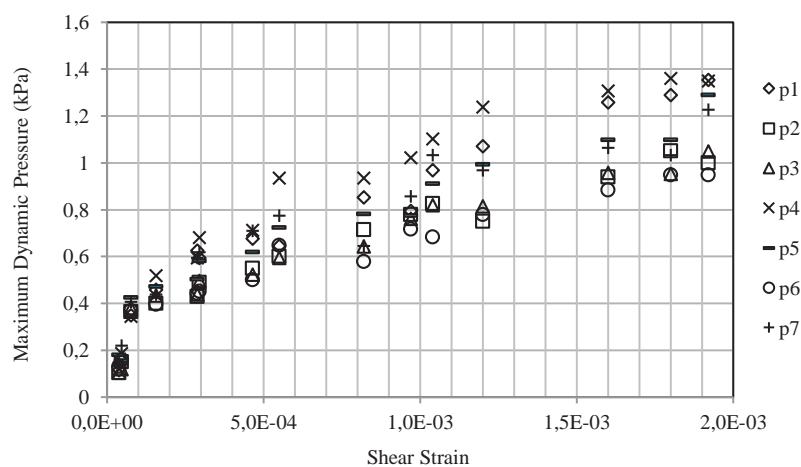| Maximum Input Acceleration (g)	0	0.05	0.07	0.11	0.17	0.22	0.26	0.30	0.35	0.40	0.45	0.50
Flexibility Ratio for *C1*	2.3	2.25	2.18	2.06	1.71	1.05	1.03	0.98	0.91	0.80	0.80	0.63
Flexibility Ratio for *C2*	0.52	0.50	0.49	0.48	0.45	0.43	0.41	0.34	0.31	0.23	0.23	0.19

Figure 11. Variation of maximum dynamic pressure with field shear strain at the culvert mid-depth for model *C1*.
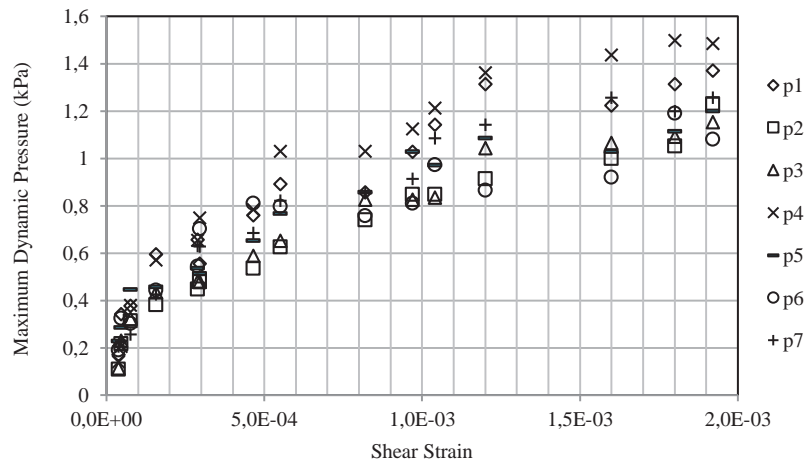
Figure 12. Variation of maximum dynamic pressure with field shear strain at the culvert mid-depth for model *C2*.

the culvert model are not constant and change during the excitation. This results in a rapidly varying pressure distribution along the sidewall of the culvert model. In order to evaluate the critical dynamic pressure distribution acting on the culvert model, the maximum bending moment at the lower slab of the culvert was calculated by considering the racking as the most critical deformation mode. Based on this analysis, the pressure distributions giving the maximum bending moments were determined. In the obtained pressure distribution there is an opposite phase angle between the recorded pressure values at same levels of the left- and right-hand sides of the culvert models, as found in the studies of Che et al. [44] and Nishiyama et al. [23]. When the upper-left corner, *UL*, of the box model is in compression, the upper-right, *UR*, corner is in tension. In contrast, when the lower-left, *LL*, corner is in tension, the lower-right corner, *LR*, is in compression, as illustrated in Fig. 13. This result can be interpreted by the cross-coupling forces that compel the culvert model to make racking deformation. Besides, it should again be noted that the "tension" forces do not represent the negative or suction

forces. It is an indication of the reduction in the static soil pressures acting on the sidewalls of the culvert.

4.7 Simplified pressure distribution

For the preliminary assessment of box-type culverts buried in dry sand, the most critical pressure distributions obtained from the shaking-table measurements were simplified, as given in Fig. 14. The peak value of the triangular dynamic pressure distribution is denoted as P_d. The P_d value was taken as the maximum pressure value measured at the upper corner of the culvert in the shaking-table tests. It was normalized with the geostatic vertical stress, $\sigma_{v,mid}$, at the mid-depth of the culvert (Eq. 6). The resulting factor was defined as the dynamic lateral pressure coefficient, k_d

$$k_d = \frac{P_d}{\sigma_{v,mid}} \qquad (6)$$

Fig. 14 shows the variation of k_d with respect to the free-field shear strain (at the mid-depth of the structure) and the maximum input acceleration for the two culvert models. The flexibility ratio of a culvert varies with the intensity of the dynamic motion. It is strongly dependent on the degraded soil shear modulus and, accordingly, on the shear strain. For this reason, the culvert models are represented by initial flexibility ratio, *IFR*, values, as given in Fig. 15. The *IFR* value is defined as the ratio of the maximum soil shear modulus to the structural racking stiffness.

The variation of k_d with respect to the shear strain and the maximum input acceleration were approximated by logarithmic and linear curves, respectively. The
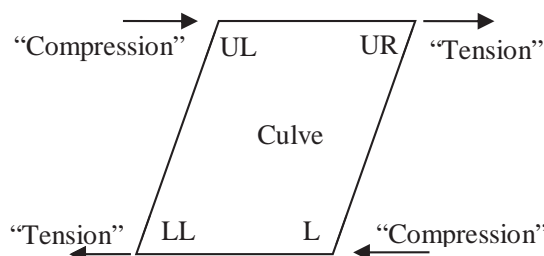

Figure 13. Schematic illustration of dynamic couple forces acting on the culvert box.

approximated equations (Eq. 7 and Eq. 8) of the curves for different *IFR* values are given as follows:

For *IFR*=2.3:

$$k_d = 0.0479 \cdot \ln(\gamma_s) + 0.5005 \quad (R^2 = 0.9659) \qquad (7)$$

For *IFR*=0.52:

$$k_d = 0.0526 \cdot \ln(\gamma_s) + 0.5505 \quad (R^2 = 0.9659) \qquad (8)$$

where a_{max} is the maximum input acceleration in g and γ_s is the free-field strain at the mid-depth of the culvert. The intensity of the shaking is better represented by the shear strain than the maximum input acceleration. Hence, it is better to estimate the dynamic lateral pressure coefficient by using the k_d versus shear strain curves shown in Fig. 15 or the corresponding approximated equations given for different *IFR* values. It should be
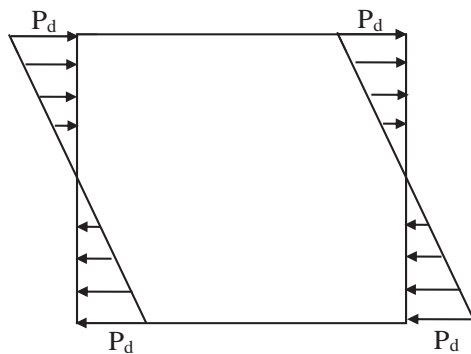
noted that the given curves are valid in the range of shear strain between 0.001% and 0.2%. Experimental validation is required for higher strains.

5. SUMMARY AND CONCLUSIONS

The aim of this study was to investigate the dynamic response of underground culverts by considering the soil–structure interaction. To achieve this, shaking-table tests were conducted on box-type models under harmonic motions. The results of the experiments were analysed in order to make an assessment of the dynamic lateral pressures acting on the underground culverts. To minimize the boundary effects, a laminar box was designed and manufactured for the shaking-table tests. Two culvert models having different aspect ratios were buried at a certain depth in a laminar container and subjected to harmonic excitations. The top and bottom thicknesses of the box models were kept thicker than the sidewalls of the box. In order to have different relative stiffness values for the box with respect to the surrounding soil, the effect of the relative stiffness on the soil's dynamic pressures was examined without considering the bending of the slabs. Pressure transducers were mounted on the right- and left-hand sides of the culvert model to measure the dynamic earth pressures. Acceleration transducers were buried in the surrounding soil to evaluate the shear strain and the acceleration response of the soil. Based on the results of the shaking-table tests, a simplified dynamic lateral coefficient was proposed to estimate the dynamic soil-pressure distribution acting on the culvert sidewalls. The major conclusions based upon an evaluation of the data obtained from the shaking table tests are summarized below:
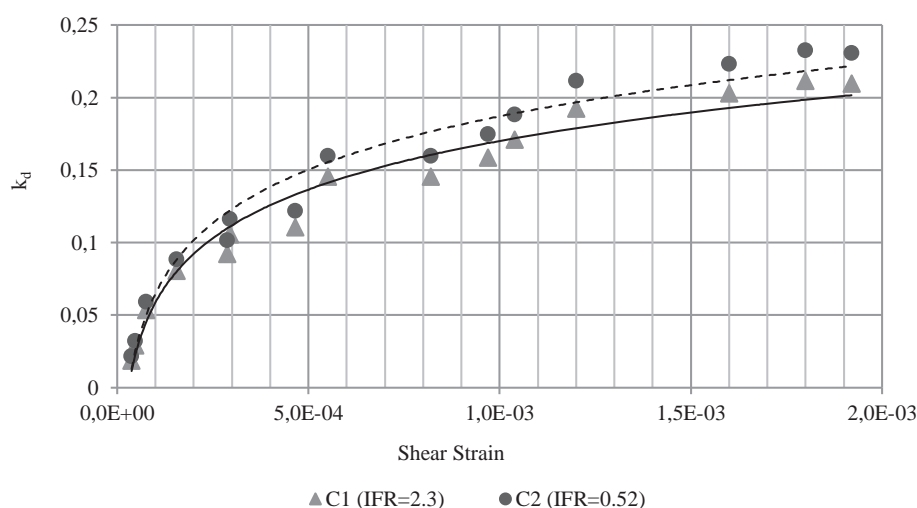

Figure 14. Simplified dynamic pressure distribution acting on the sidewalls of the culvert.

Figure 15. Variation of k_d with respect to free-field shear strain and *IFR*.

1) Static pressure values recorded at the sidewalls of the 1-g culvert models and the lateral pressure coefficient, K, calculated from these measurements were compared with the well-known at-rest pressure coefficient Ko and the active pressure coefficient, K_a. It was observed that the K values decrease with an increasing relative stiffness. The K values approach the K_o value obtained by Jaky's equation and they are larger than the K_a value.

2) Amplification of the acceleration depends on the shear strain level, which in turn is dependent upon the input motion acceleration amplitude and frequency. At low strains almost no amplification was observed in the model ground. At relatively higher strains and higher frequencies, the amplification values were between 1.2 and 1.4.

3) Dynamic pressure values recorded at the upper-left corner of the culvert model indicate an opposite phase with the lower-left and upper-right corners. In other words, when a pair of cross corners of the culvert is under dynamic compression the other pair is under dynamic tension. This behaviour indicates that the culvert model is compelled to make racking deformation by the cross-coupling forces.

4) Static and dynamic soil pressures acting on the sidewalls of the culvert were measured separately in the shaking-table tests. Based on the measurements, a dynamic pressure distribution along the sidewalls was approximated. The magnitude of the dynamic pressure distribution was normalized with the overburden pressure at the mid depth of the box-type culvert and accordingly a dynamic lateral pressure coefficient (k_d) was obtained. It was observed that the k_d value increases with a decreasing flexibility ratio and vice versa. Additionally, k_d increases logarithmically with an increasing shear strain.

5) The resonance frequencies of the ground model cannot be captured due to the limitations of the motion-generating system. The mean stresses are low due to the small scale of the box. Thus, the friction angle is higher and the soil exhibits more dilative behaviour. The proposed dynamic pressure distribution is given for box-type culverts buried in dry sand. It is necessary to perform further 1-g shaking-table tests or centrifuge tests to explore the effects of the structural dimensions and the type of soil. In this study, the range of shear-strain levels at the mid depth of the culvert varies between 0.001% and 0.2%. Further laboratory tests are needed to investigate the variation of the dynamic pressure at higher strain levels.

Acknowledgements

REFERENCES

[1] Sitar, N. 1995. (editor and coauthor with 18 members of the geotechnical reconnaissance team), Geotechnical Reconnaissance of the Effects of the January 17, 1995, HyogokenNanbu Earthquake Japan. Earthquake Engineering Research Center, University of California, Report No. 9501, 143 p.

[2] Iida, H., Hiroto, T., Yoshida, N., Iwafuji, M. 1996. Damage to Daikai Subway Station, Soils and Foundations Special Issue on Geotechnical Aspects of the January 17, 1995 HyogokenNambu Earthquake. Japanese Geotechnical Society.

[3] Parra-Montesinos, G.J., Bobet, A., Ramirez, J. 2006. Evaluation of Soil-Structure Interaction and Structural Collapse in Daikai Subway Station During Kobe Earthquake. American Concrete Institute, Structural Journal 103(1), 113-122.

[4] Wang, W.L, Wang, T.T, Su J.J, Lin, C.H., Seng, C.R. Huang, T.H. 2001. Assessment of damage in mountain tunnels due to the Taiwan Chi Chi Earthquake. Tunnel Underground Space Technology 16(3), 133-150. doi:10.1016/S0886-7798(01)00047-5

[5] Shimizu, M., Suzuki, T., Kato, S., Kojima, Y., Yashiro, K., Asakura, T. 2007. Historical Damages of Tunnels in Japan and Case Studies of Damaged Railway Tunnels in the Mid Niigata Prefecture Earthquakes. ITA-AITES World Tunnel Congress 2007, Prague, Czech Rep.

[6] Wang, Z.Z., Zhang, Z. 2013. Seismic damage classification and risk assessment of mountain tunnels with a validation for the 2008 Wenchuan earthquake. Soil Dynamics and Earthquake Engineering 45, 45-55. doi:10.1016/j.soildyn.2012.11.002

[7] Shen, Y., Gao, B., Yang, X., Tao, S. 2014. Seismic damage mechanism and dynamic deformation characteristic analysis of mountain tunnel after Wenchuan earthquake. Engineering Geology 180, 85-98. doi:10.1016/j.enggeo.2014.07.017

[8] Hashash, Y. M., Hook, J. J., Schmidt, B., I-Chiang Yao, J. 2001. Seismic design and analysis of underground structures. Tunnelling and Underground Space Technology 16, 247-293. doi:10.1016/S0886-

7798(01)00051-7

[9] Duke, C.M., Leeds, D.J. 1959. Effects of Earthquakes on Tunnels, Protective Construction in a Nuclear Age. Proceedings 2nd Protective Construction Symp. March 24-26, pp. 303-328.

[10] Stevens, P.R. 1977. A review of the effects of earthquakes on underground mines. US Energy Research and Development Administration United States Geological Survey Open File, Report No. 77313, 47p.

[11] Dowding, C.H., Rozen, A. 1978. Damage to rock tunnels from earthquake shaking. J. Geotech. Eng. Div. ASCE 104(2), 175-192.

[12] Owen, G.N., Scholl, R.E. 1981. Earthquake engineering of large underground structures. Federal Highway Administration and National Science Foundation, Report no. FHWA_RD80_195.

[13] Sharma, S., Judd, W.R. 1991. Underground opening damage from earthquakes. Engineering Geology 30, 263-276. doi:10.1016/0013-7952(91)90063-Q

[14] Power, M., Rosidi, D., Kaneshiro, J. 1998. Seismic vulnerability of tunnels and underground structures revisited. Proceedings of the North American Tunneling Conference. Elsevier, Long Beach, CA, USA.

[15] Kaneshiro, J.Y., Power, M., Rosidi, D. 2000. Empirical correlations of tunnel performance during earthquakes and aseismic aspects of tunnel design. Proceedings of the Conference on Lessons Learned From Recent Earthquakes-On Earthquakes in Turkey 1999, November 8-11.

[16] Wang, J.N. 1993. Seismic Design of Tunnels: A State of the Art Approach. Monograph 7, Parsons, Brinckerhoff, Quade and Douglas Inc., New York.

[17] Penzien, J. 2000. Seismically induced racking of tunnel linings. Earthquake Engineering & Structural Dynamics 29(5), 683-691. doi:10.1002/(SICI)1096-9845(200005)29:5<683::AID-EQE932>3.0.CO;2-1

[18] Huo, H., Bobet, A., Fernandez, G., Ramirez, J. 2006. Analytical solution for deep rectangular underground structures subjected to far field shear stresses. Tunneling and Underground Space Technology 21, 613–625. doi:10.1016/j.tust.2005.12.135

[19] Bobet, A., Fernández, G., Huo, H., Ramírez, J. 2008. A practical iterative procedure to estimate seismic induced deformations of shallow rectangular structures. Canadian Geotechnical Journal 45, 923-938.

[20] Okabe, S. 1926. General theory of earth pressures, Journal of the Japan Society of Civil Engineering 12(1).

[21] Mononobe, H.A., Matsuo, H. 1929. On the determination of earth pressures during earthquakes.

Proceedings of World Engineering Congress, Tokyo, Japan, pp. 177-185.

[22] Luu, A.L. 2013. Seismic earth pressures measured during a shake table experiment of underground structures. M. Sc. Thesis, University of California, Irvine.

[23] Nishiyama, S., Kawawa, I., Muroya, K., Haya, H., Nishimura, A. 2000. Experimental study of seismic behavior of box type tunnel constructed by open cutting method. Twelfth World Conference on Earthquake Engineering, January 30-February 4, Auckland, New Zealand.

[24] Che, A., Iwatate, T. 2002. Shaking table test and numerical simulation of seismic response of subway structures, Structures under shock and impact VII 367-376.

[25] Matsui, J., Ohtomo, K., Kanaya, K. 2004. Development and Validation of Nonlinear Dynamic Analysis in Seismic Performance Verification of Underground RC Structures, Journal of Advanced Concrete Technology 2(1), 25-35.

[26] Che, A., Iwatate, T., Ge, X. 2006a. Study on dynamic response of embedded long span corrugated steel culverts using scaled model shaking table tests and numerical analyses. Journal of Zhejiang University Science A 7(3), 430-435.

[27] Moss, R.E.S, Crosariol, V. A. 2013. Scale model shake table testing of an underground tunnel cross section in soft clay. Earthquake Spectra 29(4), 1413-1440. doi: http://dx.doi.org/10.1193/070611EQS162M

[28] Chen, G., Chen, S., Zuo, X., Du, X., QI, C., Wang, Z. 2014. Shaking-table tests and numerical simulations on a subway structure in soft soil. Soil Dynamics and Earthquake Engineering 76, 13-28. doi:10.1016/j.soildyn.2014.12.012.

[29] Cilingir, U., Madabhushi, S.P.G. 2011a. Effect of depth on the seismic response of circular tunnels. Canadian Geotechnical Journal 48(1), 117-127.

[30] Cilingir, U., Madabhushi, S.P.G. 2011b. A model study on the effects of input motion on the seismic behavior of tunnels. Soil Dynamics and Earthquake Engineering 31, 452-462. doi:10.1016/j.soildyn.2010.10.004

[31] Lanzano, G., Bilotta, E., Russo, G., Silvestri, F., Madabhushi, S.P.G. 2012. Centrifuge modeling of seismic loading on tunnels in sand. Geotechnical Testing Journal 35, 854-869.

[32] Cilingir, U., Madabhushi, S.P.G. 2011c. Effect of depth on the seismic response of square tunnels. Soils and Foundations 51(3), 449-457. http://doi.org/10.3208/sandf.51.449

[33] Pitilakis, K., Tsinidis, G., Anastisiadis, A., Pitilakis, D., Heron, C., Madabushi, S.P.G., Stringer,

M., Paolucci, R. 2013. Ivestigation of Several Aspects Affecting the Seismic Behaviour of Shallow Rectangular Underground Structures in Soft Soils, 2013. Series Project Web: http://www.series.upatras.gr/sites/default/files/file/SERIES_TUNNELSEIS_Final_Report.pdf

[34] Dashti, S., Hushmand, A., Ghayoomi, M., McCartney, J.S., Zhang, M., Hushmand, B., Mokarram, N., Bastani, A., Davis, C., Yangsoo, L., Hu, J. 2013. Centrifuge Modeling of Seismic Soil-Structure-Interaction and Lateral Earth Pressures for Large Near-Surface Underground Structures. Proceedings of the 18th International Conference on Soil Mechanics and Geotechnical Engineering, Paris, France.

[35] Çalısan, O. 1999. A Model Study on the Seismic Behavior of Gravity Retaining Walls. Ph.D Dissertation, Middle East Technical University, Ankara.

[36] Prasad, S.K., Towhata, I., Chandradhara, G.P., Nanjundaswamy, P. 2004. Shaking table tests in earthquake geotechnical engineering. Current Science Special section: Geotechnics and earthquake hazards 87(10), 1398-1404.

[37] Turan, A., Hinchberger, S., El Naggar, H. 2009. Design and commissioning of a laminar soil container for use on small shaking tables. Soil Dynamics and Earthquake Engineering 29(2), 404-414. doi:10.1016/j.soildyn.2008.04.003

[38] Hokmabadi, A.S. 2014. Effect of dynamic soil-pile-structure interaction on seismic response of mid-rise moment resisting frames. Ph. D. Dissertation, Faculty of Engineering and Information Technology, University of Technology Sydney, Sydney, Australia.

[39] Hardin, B.O., Drnevich, V.P. 1972. Shear modulus and damping in soils: design equation and curves. J. Soil Mech. Found. Engng. Div. 98(7), 667–692.

[40] Darendeli, M. 2011. Development of a new family of normalized modulus reduction and material damping curves. Ph.D. Thesis, Dept. of Civil Eng., Univ. of Texas, Austin.

[41] Okamoto, M., Fityus, S. 2006. An Evaluation of the Dry Pluviation Preparation Technique Applied to Silica Sand Samples. Geomechanics and Geotechnics of Particulate Media: Proceedings of the International Symposium on Geomechanics and Geotechnics of Particulate Media, London, pp. 33–34.

[42] Jaky, J. 1948. Pressure in soils, 2nd ICSMFE, London, Vol. 1, pp. 103-107.

[43] Rankine, W. 1857. On the stability of loose earth Philosophical Transactions of the Royal Society of London 147, 9-27.

[44] Che, A., Iwatate, T., Ge, X. 2006b. Evaluation of dynamic soil structure interaction and dynamic seismic soil pressures acting on it subjected to strong earthquake motions. Journal of Shangai Jiaotong University 11(4), 530-536.